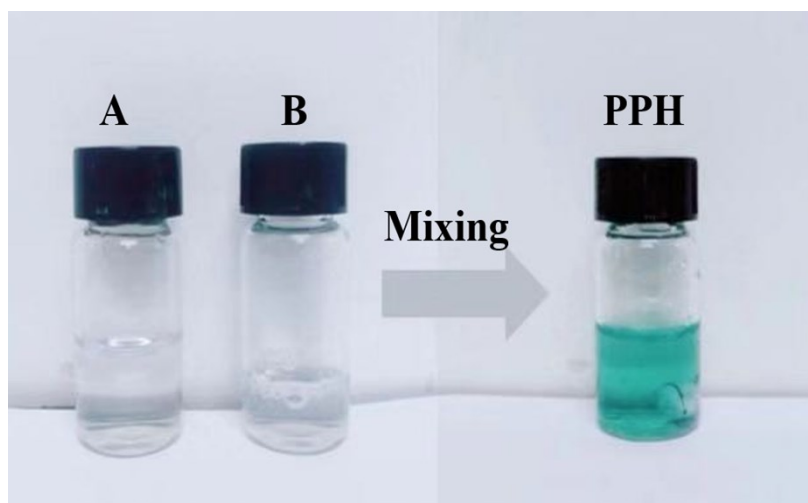


## **Nickel nanocrystal/nitrogen-doped carbon composites as efficient and carbon monoxide-resistant electrocatalysts for methanol oxidation reaction**

*Na Wu,<sup>a,b</sup> Meixu Zhai,<sup>a</sup> Fei Chen,<sup>a</sup> Xue Zhang,<sup>a</sup> Ruihong Guo,<sup>a</sup> Tuoping Hu,<sup>\*a</sup> Mingming Ma<sup>\*a,c</sup>*

- a. Department of Chemistry, College of Science, North University of China, Taiyuan, Shanxi 030051, China*
- b. Department of Chemistry and Chemical Engineering, Lvliang University, Lvliang, Shanxi 033001, China*
- c. CAS Key Laboratory of Soft Matter Chemistry, Hefei National Laboratory for Physical Sciences at the Microscale, University of Science and Technology of China, Hefei, Anhui 230026, China*

<sup>\*</sup>Correspondence: hutuopingsx@126.com, mma@ustc.edu.cn



**Fig. S1.** The photographs of polyaniline-polyvinyl alcohol hydrogel synthesis. Immediately after mixing solution A and B, the mixture turns into blue color, indicating the formation of polyaniline.

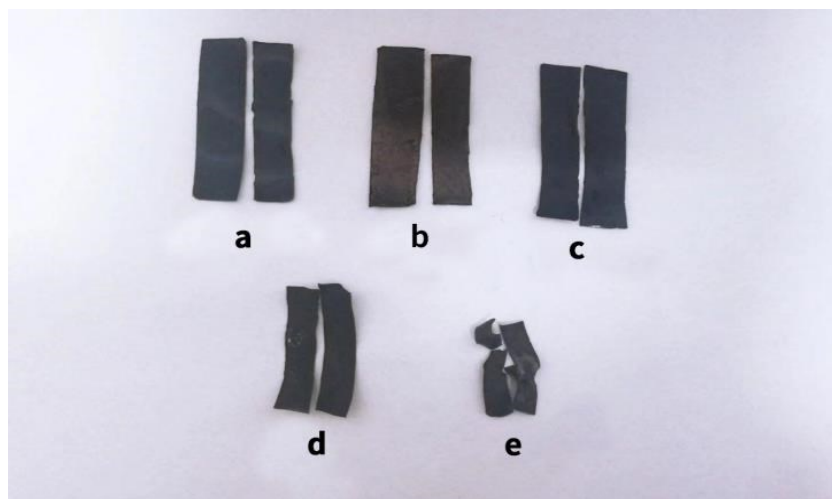


**Fig. S2.** The photographs of samples during the five synthesis steps. a) as-prepared PPH hydrogel; b) after ammonia solution treatment; c) after absorption of  $\text{NiCl}_2$  salt; d) after freeze-drying; e) after calcination.

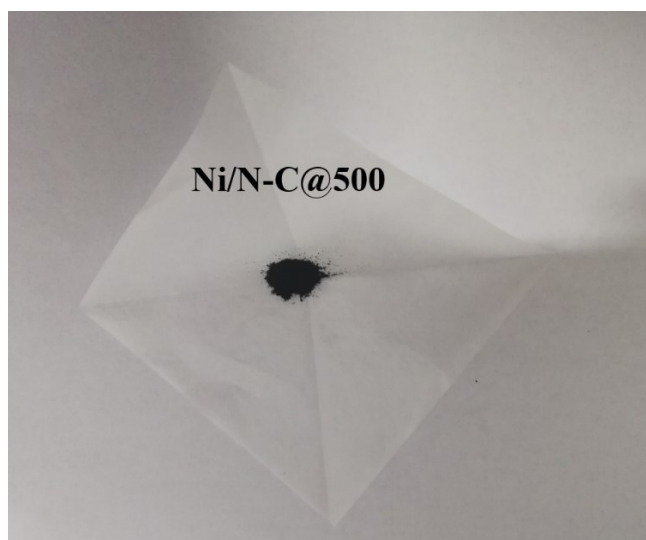


**Fig. S3.** The photograph of Ni/N-C@500 powders.

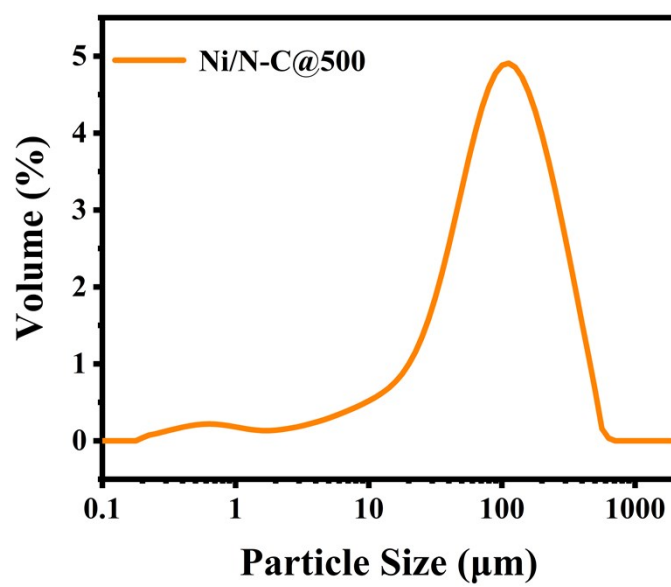


**Fig. S4.** The particle size distribution of Ni/N-C@500.

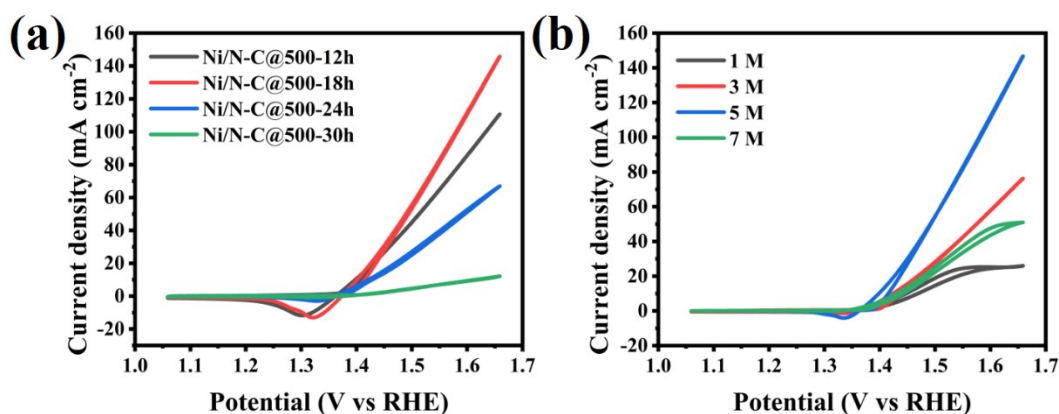


**Fig. S5.** CV curves of the electrocatalysts prepared (a) with different soaking time and (b) with different concentration of nickel chloride solution. The CV curves were measured at  $10 \text{ mV s}^{-1}$  in  $1 \text{ mol L}^{-1}$  KOH and  $1.0 \text{ mol L}^{-1}$  methanol.

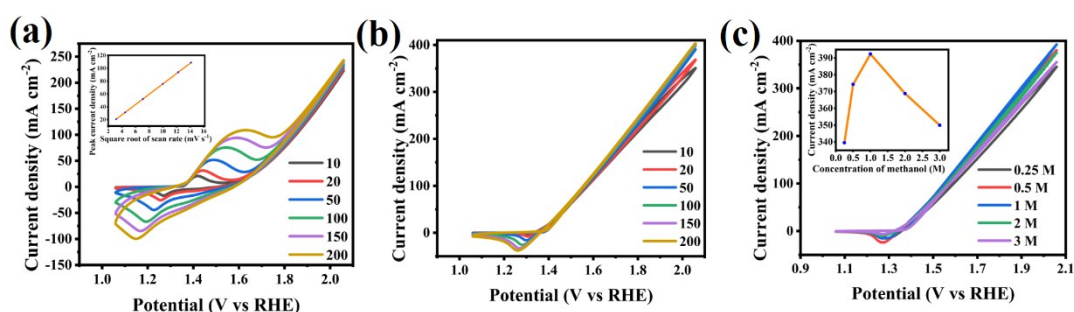


**Fig. S6.** Electrochemical characterization of Ni/N-C@500 in different electrolyte solutions. (a) CV curves of Ni/N-C@500 in  $1 \text{ M}$  KOH and (b) in  $1 \text{ M}$  KOH with  $1 \text{ M}$  methanol at different scan rate ( $10\text{--}200 \text{ mV s}^{-1}$ ). Inset of (a) shows the relation between the oxidation peak current and the square root of the scan rate. (c) CV curves of Ni/N-C@500 in  $1 \text{ M}$  KOH solution with different concentration of methanol ( $0.25\text{--}3 \text{ M}$ , scan rate:  $50 \text{ mV s}^{-1}$ ). Inset of (c) shows the relation between the oxidation peak current and the different concentration of methanol.

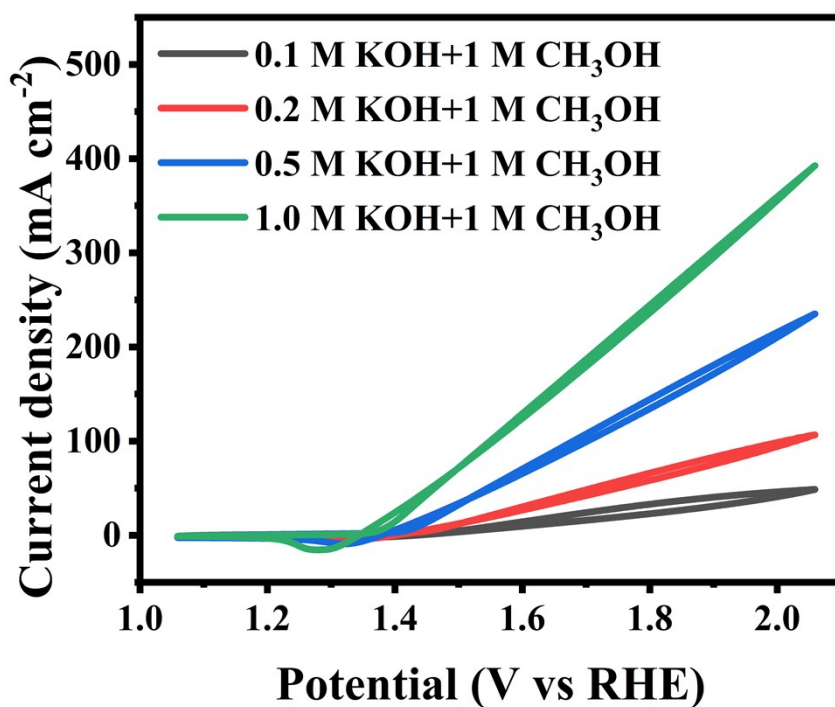


**Fig. S7.** CV curves of Ni/N-C@500 in 1 M methanol solution with different concentration of KOH (0.1-1 M, scan rate: 50 mV s<sup>-1</sup>).

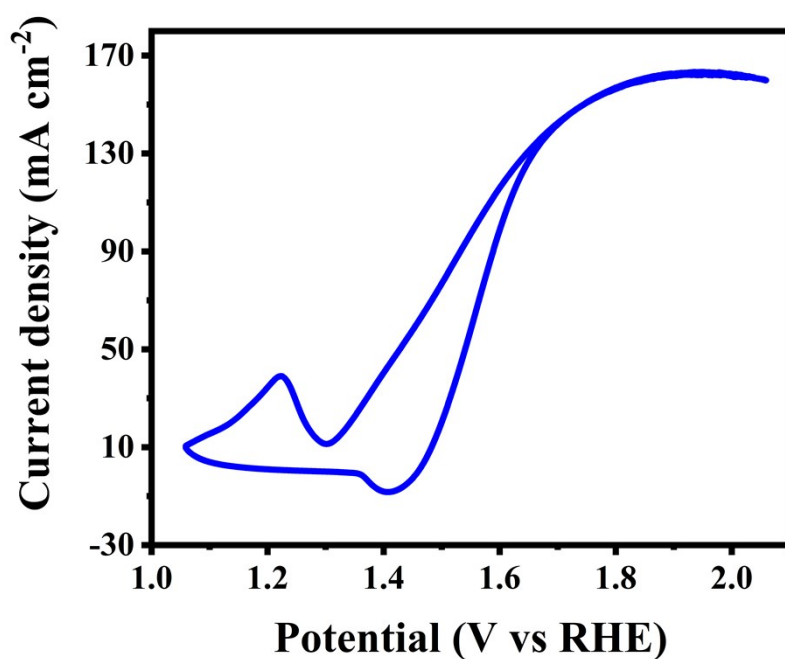


**Fig. S8.** CV curve of Ni/N-C@500 in 1M KOH and 1 M methanol solution subtracts the CV curve of Ni/N-C@500 in 1M KOH (scan rate: 50 mV s<sup>-1</sup>).

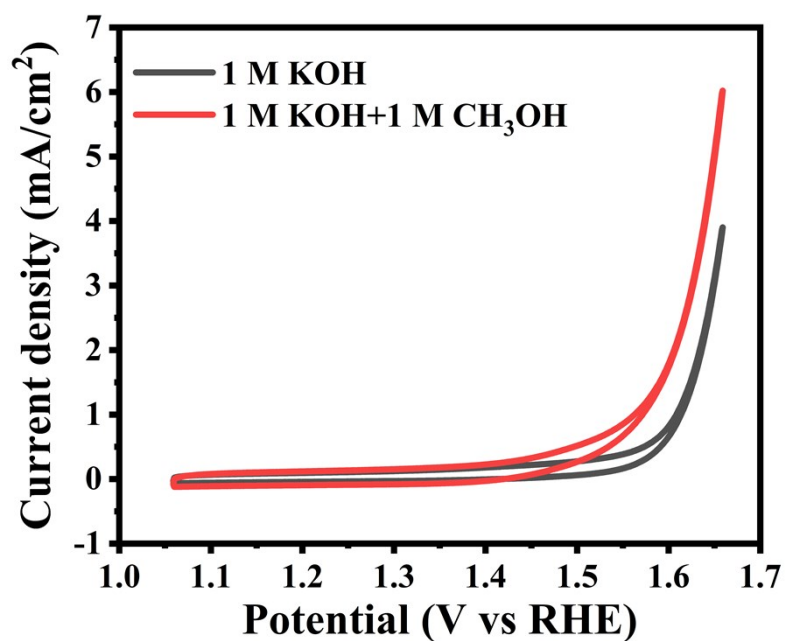


**Fig. S9.** CV curves of the N-C@500 in 1 M KOH and 1 M methanol solution.

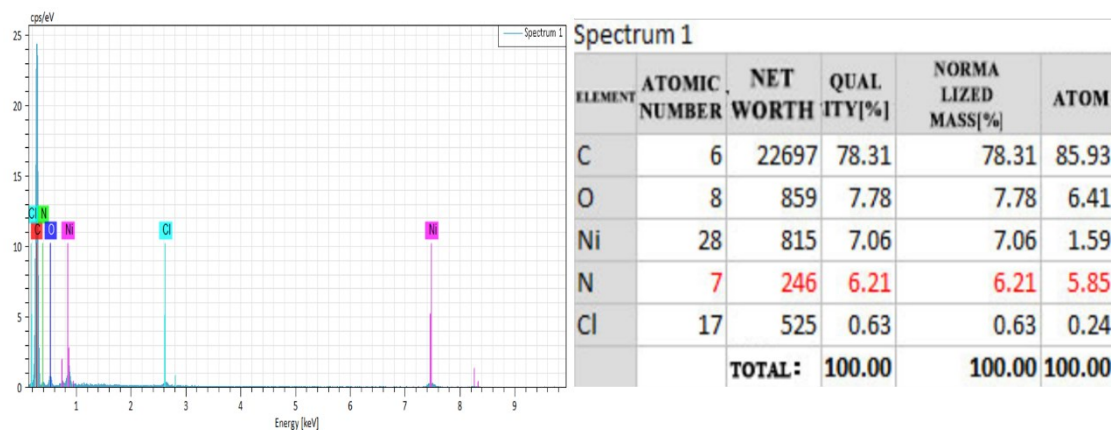


**Fig. S10.** EDS spectra of Ni/N-C@500.

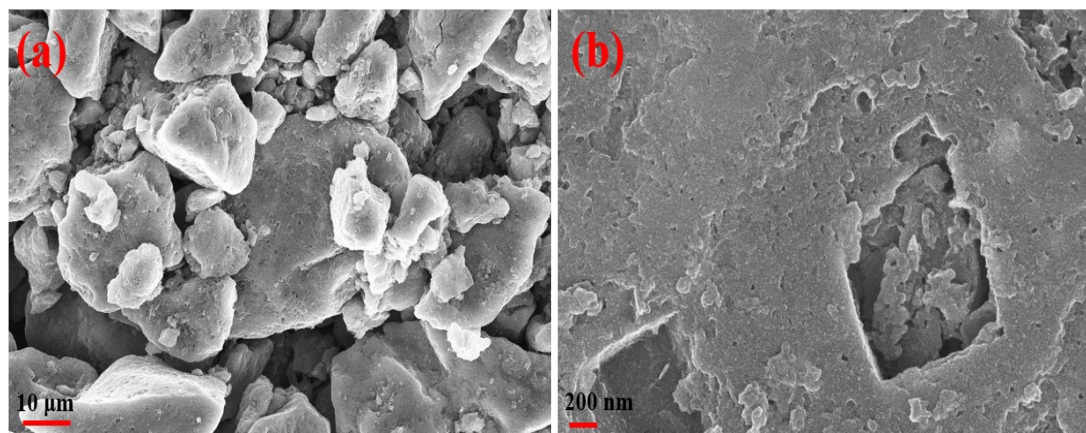


**Fig. S11.** SEM images of Ni/N-C@500 electrocatalyst after 12-h MOR test.

**Table S1.** Comparison of the Ni/N-C composites prepared at different pyrolysis temperatures.

pyrolysis temperature (°C)	current density for MOR (mA cm <sup>-2</sup> )	C <sub>dl</sub> (mF cm <sup>-2</sup> )	ECSA
400	73.5	3.2	80
500	147	4.29	107
600	97.6	3.62	90.5

The current densities were taken at a fixed potential of 0.6 V vs SCE.